

Peng Feng, Lu Wang, Michael Brown, Songjie Wang, and Xiawen Li, 2019, Separating multiple episodes of partial melting in polyorogenic crust: An example from the Haiyangsuo complex, northern Sulu belt, eastern China: *GSA Bulletin*, <https://doi.org/10.1130/B35210.1>.

Data Repository

Figure DR1. Harker diagrams of major oxide compositions of four granite gneisses, four leucosomes, four metabasites and four leucogranites, from TABLE DR1.

Figure DR2. Harker diagrams of trace element compositions of four granite gneisses, four leucosomes, four metabasites and four leucogranites, from TABLE DR1.

Figure DR3. Box and whisker plots showing the distribution of temperatures calculated using Ti-in-zircon thermometry at 1 GPa for the zircon rims from the granite gneisses (A), the zircon cores/mantles and rims from the leucosomes (B), the magmatic zircon rims/new grains from the metabasites (C), and the zircon mantles and rims from the leucogranites (D). The box represents the interquartile range (the middle 50% of the data from the 25th to the 75th percentile), the open circles in (B, C) represent suspected outliers. The 25th and 75th percentile temperatures are given at the bottom and top of the box, respectively.

TABLE DR1. Chemical compositions of the granite gneisses, leucosomes, metabasites, and leucogranites from the Haiyangsuo complex, northern Sulu belt.

TABLE DR2. LA-ICPMS U–Pb isotope compositions of zircon from the granite gneisses, leucosomes, metabasites, and leucogranites in the Haiyangsuo complex.

TABLE DR3. Trace element compositions of zircon from the granite gneisses, leucosomes, metabasites, and leucogranites.

TABLE DR4. Lu-Hf isotope compositions of zircon from the granite gneisses, leucosomes, metabasites, and leucogranites.

TABLE DR5. Composition of phengite in the leucogranites.

ANALYTICAL METHODS

Whole-rock Major and Trace Element Analysis

For determination of whole rock major and trace element concentrations, fresh and homogeneous whole-rock samples were pulverized to less than 200 mesh using an agate ring mill. Major element concentrations were determined by X-ray fluorescence spectrometer (XRF-1800) on fused glass discs in the Hubei Geological Research Laboratory, following the procedure described by Ma et al. (2012).

Whole-rock trace element concentrations were determined using an Agilent 7700e ICP-MS at the Wuhan Sample Solution Analytical Technology Co. Ltd., Wuhan, China. The detailed sample-digestion procedure (Liu et al., 2008a) was as follows: (1) sample powders (–200 mesh) were placed in an oven at 105 °C for 12 h to dry; (2) 50 mg of each sample powder was accurately weighed and placed in a Teflon bomb; (3) 1 ml HNO₃ and 1 ml HF were slowly added to the Teflon bomb, which was put in a stainless steel pressure jacket and heated to 190 °C in an oven for >24 h; (4) after cooling, the Teflon bomb was opened, placed on a hotplate at 140 °C and evaporated to incipient dryness, and then 1 ml HNO₃ was added and evaporated to dryness again; (5) 1 ml of HNO₃, 1 ml of MQ water and 1 ml internal standard solution of 1ppm In were added, and the Teflon bomb was resealed and placed in the oven at 190 °C for >12 h; and, (6) the final solution was transferred to a polyethylene bottle and diluted to 100 g by the addition of 2% HNO₃.

Zircon U-Pb Isotope and Trace Element Analysis

U-Pb isotope and trace element analysis of zircon was conducted simultaneously by LA-ICP-MS (at the Wuhan Sample Solution Analytical Technology Co. Ltd., Wuhan, China) following the same operating conditions and data reduction protocols as those described by Zong et al. (2017). This laboratory uses a GeolasPro laser ablation system, comprising a COMPexPro 102 ArF excimer laser and a MicroLas optical system, coupled with an Agilent 7700e ICP-MS instrument to acquire ion-signal intensities. Helium was used as a carrier gas and argon was used as the make-up gas, which was mixed with the carrier gas via a T-connector before entering the ICP. In this study, the spot size and frequency of the laser were set to 24 μm and 5Hz, respectively. Each analysis incorporated a background acquisition of ~20–30 s followed by 50 s of data acquisition from the zircon. For U-Pb analysis, zircon standard 91500 was used as an external standard, and zircon standards GJ-1 and Ple were used as unknown samples to monitor the stability and accuracy of the age data. For calibration of the trace element analyses, we used glass NIST610 as an external standard and Si as an internal standard; zircon standards 91500 and GJ-1 were used to monitor the quality of the analyses. The software ICPMSDataCal was used to perform off-line selection and integration of background and analyte signals, time-drift correction and quantitative calibration for U-Pb geochronology and trace element concentrations (Liu et al., 2008b, 2010). Concordia diagrams and weighted mean age calculations were made using Isoplot (Ludwig, 2003).

Zircon Lu–Hf Isotope Analysis

Zircon Lu–Hf isotope analysis was undertaken using LA-MC-ICP-MS at the State Key Laboratory of Geological Processes and Mineral Resources (GPMR), China University of Geosciences, Wuhan. Sampling was performed on the same locations analyzed for U–Pb isotope ratios and trace element concentrations using an excimer laser ablation system (GeoLas 2005) with a spot size and frequency set to 44 μm and 8 Hz, respectively. Helium was used as a carrier gas. A Plasma HR MC-ICP-MS instrument (Nu Instruments Ltd., UK) was used to acquire time-resolved signals following the same instrumental parameters for the laser-ablation system and analytical protocols for the MC-ICP-MS as described by Yuan et al. (2008). Each of the zircon standards 91500 ($^{176}\text{Hf}/^{177}\text{Hf} = 0.282308 \pm 0.000006$ (2σ); Blichert-Toft, 2008), GJ-1 ($^{176}\text{Hf}/^{177}\text{Hf} = 0.282000 \pm 0.000006$ (2σ); Morel et al., 2008) and Monastery ($^{176}\text{Hf}/^{177}\text{Hf} = 0.282739 \pm 0.000026$ (2σ); Woodhead and Hergt, 2005) was analyzed after every ten unknowns; 91500 was used as an external standard, whereas GJ-1 and Monastery were analyzed as unknowns. The Hf isotope compositions obtained in this study are: 0.282307 ± 0.000007 (2σ , $N = 32$) for 91500, 0.282007 ± 0.000024 (2σ , $N = 12$) for GJ-1 and 0.282721 ± 0.000022 (2σ , $N = 11$) for Monastery, respectively. Data reduction followed the protocol summarized by Liu et al. (2010). The software ICPMSDataCal was used to perform off-line selection and integration of background and analyte signals, interference and mass fractionation corrections and external calibration of Lu–Hf isotope ratios (cf. Liu et al., 2010).

Whole-rock Sr–Nd Isotope Analysis

Whole-rock Sr–Nd isotope ratios were obtained using a Finnigan Triton thermal ionization mass spectrometer at GPMR, China University of Geosciences, Wuhan. The sample preparation, chemical separation and analytical procedures for Sr and Nd isotope analysis are similar to those given by Gao et al. (2004) and Ling et al. (2009). The $^{87}\text{Rb}/^{86}\text{Sr}$ and $^{147}\text{Sm}/^{144}\text{Nd}$ ratios of the samples were calculated from Rb, Sr, Sm and Nd concentrations measured using an Agilent 7500a ICP-MS. The total analytical blanks were 200–500 pg for Rb and Sr, and 50 pg for Sm and Nd. The measured Sr and Nd isotope ratios were normalized to $^{86}\text{Sr}/^{88}\text{Sr} = 0.1194$ and $^{146}\text{Nd}/^{144}\text{Nd} = 0.7219$, respectively. During the course of analysis, results obtained for the Sr isotope standard SRM NBS987 (Thirlwall, 1991) gave an average $^{87}\text{Sr}/^{86}\text{Sr}$ value of 0.710238 ± 0.00011 (2σ , $N = 17$) and for the Nd isotope standard JNdi-1 (Tanaka et al., 2000) gave an average $^{143}\text{Nd}/^{144}\text{Nd}$ of 0.512122 ± 0.000007 (2σ , $N = 16$). The 2σ errors we report below on the initial $^{87}\text{Sr}/^{86}\text{Sr}$ ratios and $\epsilon_{\text{Nd}}(t)$ were calculated using the procedures described by Wu et al. (2015).

Electron Probe Micro-analysis, X-ray Energy-dispersive Spectroscopy Analysis and Zircon Cathodoluminescence Imaging

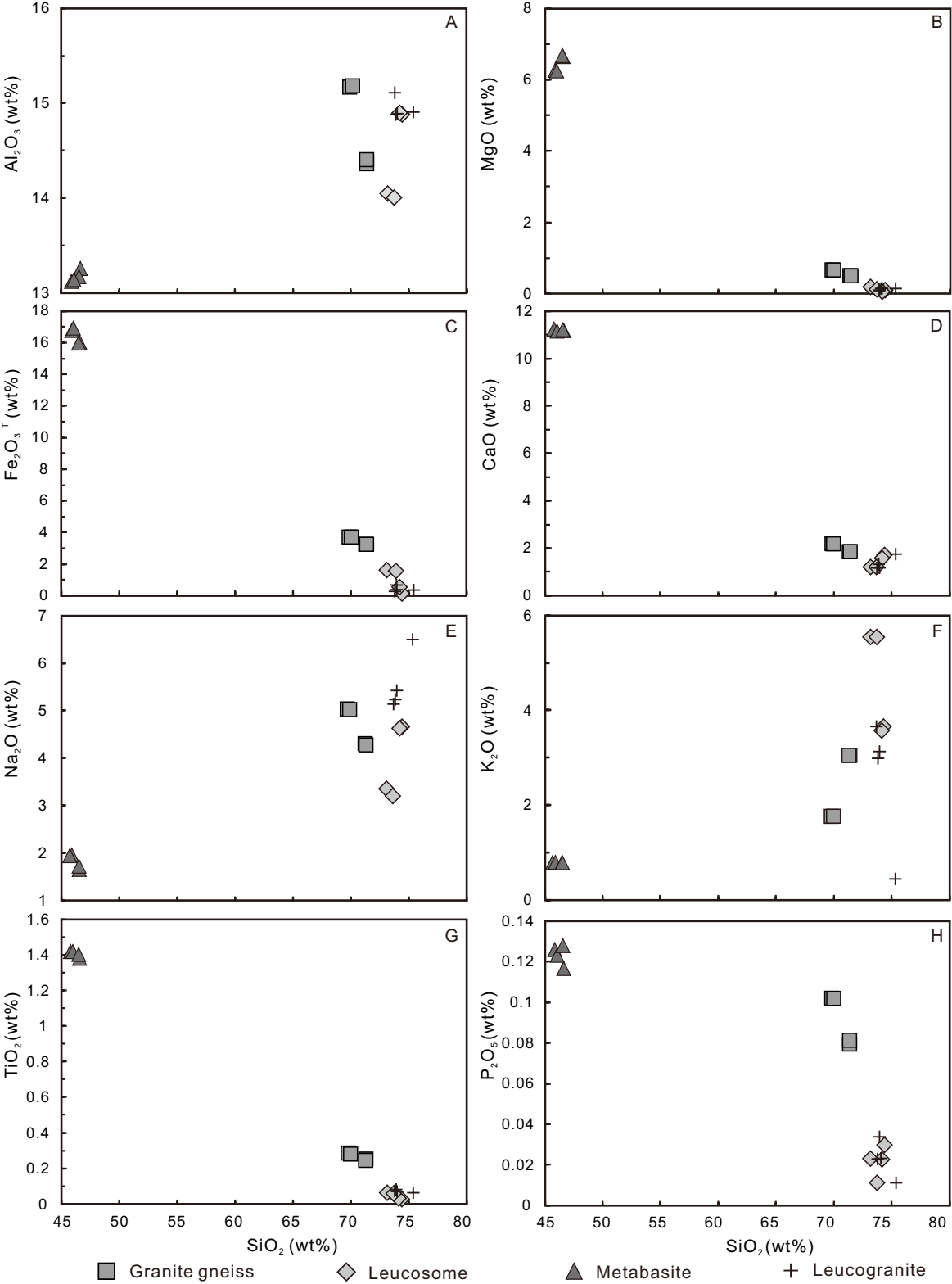
Major element compositions of phengite in leucogranite dikes were determined using a JEOL JXA-8230 electron probe micro-analyzer at the Center for Global Tectonics, School of Earth Sciences, China University of Geosciences, Wuhan. The following operating conditions were used: 15 kV accelerating voltage, 20 nA beam current, a 1–5 mm micron beam diameter and a count time of 15–20 s. Standard minerals from SPI Supplies Inc. were used as standards and raw X-ray intensities were corrected using a ZAF algorithm. The detailed operating conditions and procedures were described in Wang et al. (2019).

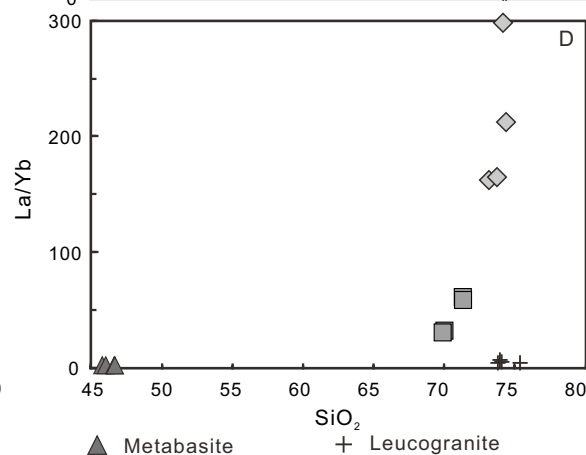
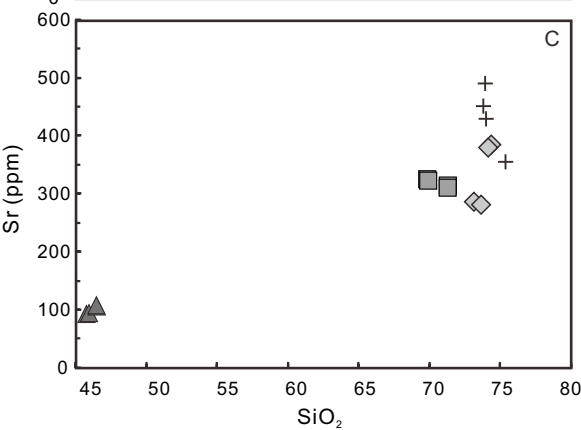
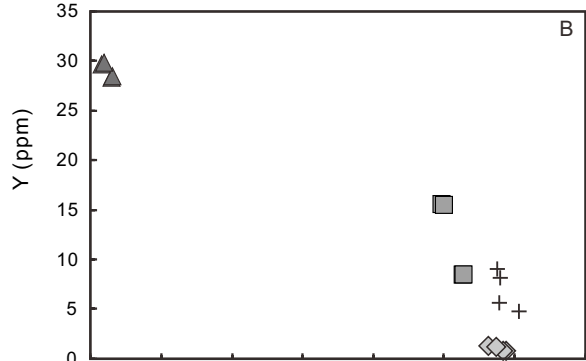
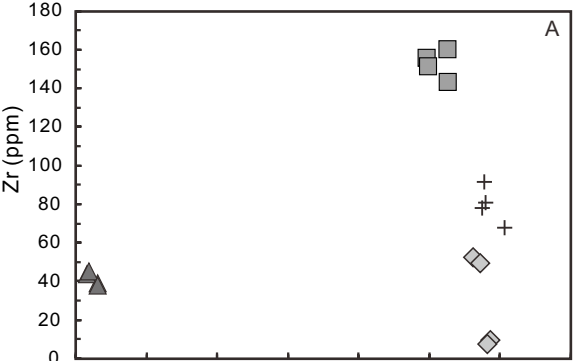
Backscattered electron imaging, X-ray energy dispersive spectroscopy for mineral identification and zircon cathodoluminescence (CL) imaging were collected at the GPMR, China University of Geosciences, Wuhan, using a FEI Quanta 450 field emission gun scanning electron microscope (SEM) with an attached Oxford SDD Inca X-Max 50 energy dispersive spectroscopy and Gatan Mono CL4⁺ CL system. The working conditions for SEM imaging were 20 kV with a spot size of ~6.0 mm and working distance of ~12 mm. For zircon CL imaging, the working conditions were set to be 10 kV with a spot size of ~5 mm and working distance of ~14 mm.

REFERENCES CITED

- Blichert-Toft, J., 2008, The Hf isotopic composition of zircon reference material 91500: *Chemical Geology*, v. 253, p. 252–257, <https://doi.org/10.1016/j.chemgeo.2008.05.014>.
- Gao, S., Rudnick, R.L., Yuan, H.L., Liu, X.M., Liu, Y.S., Xu, W.L., Ling, W.L., Ayers, J., Wang, X.C., and Wang, Q.H., 2004, Recycling lower continental crust in the North China craton: *Nature*, v. 432, no. 7019, p. 892–897, <https://doi.org/10.1038/nature03162>.
- Ling, W.L., Duan, R.C., Xie, X.J., Zhang, Y.Q., Zhang, J.B., Cheng, J.P., Liu, X.M., and Yang, H.M., 2009, Contrasting geochemistry of the Cretaceous volcanic suites in Shandong province and its implications for the Mesozoic lower crust delamination in the eastern North China craton: *Lithos*, v. 113, p. 640–658, <https://doi.org/10.1016/j.lithos.2009.07.001>.
- Liu, Y.S., Zong, K.Q., Kelemen, P.B., and Gao, S., 2008a, Geochemistry and magmatic history of eclogites and ultramafic rocks from the Chinese continental scientific drill hole: Subduction and ultrahigh-pressure metamorphism of lower crustal cumulates: *Chemical Geology*, v. 247, no. 1–2, p. 133–153, <https://doi.org/10.1016/j.chemgeo.2007.10.016>.
- Liu, Y.S., Hu, Z.C., Gao, S., Günther, D., Xu, J., Gao, C.G., and Chen, H.H., 2008b, In situ analysis of major and trace elements of anhydrous minerals by LA-ICP-MS without applying an internal standard: *Chemical Geology*, v. 257, p. 34–43, <https://doi.org/10.1016/j.chemgeo.2008.08.004>.
- Liu, Y.S., Gao, S., Hu, Z.C., Gao, C.G., Zong, K.Q., and Wang, D.B., 2010, Continental and oceanic crust recycling-induced melt–peridotite interactions in the Trans-North China Orogen: U-Pb dating, Hf isotopes and trace elements in zircons from mantle xenoliths: *Journal of Petrology*, v. 51, p. 537–571, <https://doi.org/10.1093/petrology/egp082>.

- Ludwig, K., 2003, User's manual for ISOPLOT/EX, version 3. A geochronological toolkit for Microsoft Excel: Berkeley Geochronology Center Special Publication (4).
- Ma, Q., Zheng, J., Griffin, W.L., Zhang, M., Tang, H., Su, Y., and Ping, X., 2012, Triassic "adakitic" rocks in an extensional setting (North China): Melts from the cratonic lower crust: *Lithos*, v. 149, p. 159–173, <https://doi.org/10.1016/j.lithos.2012.04.017>.
- Morel, M.L.A., Nebel, O., Nebel-Jacobsen, Y.J., Miller, J.S., and Vroon, P.Z., 2008, Hafnium isotope characterization of the GJ-1 zircon reference material by solution and laser-ablation MC-ICPMS: *Chemical Geology*, v. 255, p. 231–235, <https://doi.org/10.1016/j.chemgeo.2008.06.040>.
- Tanaka, T., Togashi, S., Kamioka, H., Amakawa, H., Kagami, H., Hamamoto, T., and Dragusanu, C., 2000, JNdi-1: a neodymium isotopic reference in consistency with LaJolla neodymium: *Chemical Geology*, v. 168, no. 3–4, p. 279–281, [https://doi.org/10.1016/S0009-2541\(00\)00198-4](https://doi.org/10.1016/S0009-2541(00)00198-4).
- Thirlwall, M.F., 1991, Long-term reproducibility of multicollector Sr and Nd isotope ratio analysis: *Chemical Geology*, v. 94, no. 2, p. 85–104, [https://doi.org/10.1016/S0009-2541\(10\)80021-X](https://doi.org/10.1016/S0009-2541(10)80021-X).
- Wang, J.P., Li, X.W., Ning, W.B., Kusky, T., Wang, L., Polat, A., and Deng, H., 2019, Geology of a Neoproterozoic suture: Evidence from the Zunhua ophiolitic mélange of the Eastern Hebei Province, North China Craton: *Geological Society of America Bulletin*, <https://doi.org/10.1130/B35138.1>.
- Woodhead, J.D., and Hergt, J.M., 2005, A preliminary appraisal of seven natural zircon reference materials for in situ Hf isotope determination: *Geostandards and Geoanalytical Research*, v. 29, p. 183–195, <https://doi.org/10.1111/j.1751-908X.2005.tb00891.x>.
- Wu, Y.C., Yang, Y.H., and Yang, J.H., 2015, Error calculation of radiogenic geochemical parameters in isotopic geology: a case study of Hf-Nd-Sr isotopes: *Geochimica*, v. 44, p. 600–607, <https://doi.org/10.3969/j.issn.0379-1726.2015.06.009>.
- Yuan, H.L., Gao, S., Dai, M.N., Zong, C.L., Günther, D., Fontaine, G.H., Liu, X.M., and Diwu, C.R., 2008, Simultaneous determinations of U-Pb age, Hf isotopes and trace element compositions of zircon by excimer laser-ablation quadrupole and multiple-collector ICP-MS: *Chemical Geology*, v. 247, p. 100–118, <https://doi.org/10.1016/j.chemgeo.2007.10.003>.
- Zong, K.Q., Klemm, R., Yuan, Y., He, Z.Y., Guo, J.L., Shi, X.L., Liu, Y.S., Hu, Z.C., and Zhang, Z.M., 2017, The assembly of Rodinia: The correlation of early Neoproterozoic (ca. 900 Ma) high-grade metamorphism and continental arc formation in the southern Beishan Orogen, southern Central Asian Orogenic Belt (CAOB): *Precambrian Research*, v. 290, p. 32–48, <https://doi.org/10.1016/j.precamres.2016.12.010>.





■ Granite gneiss

◇ Leucosome

▲ Metabasite

+ Leucogranite

